Shape optimisation of concrete open spandrel arch bridges

Article *in* Gradevinar · December 2015

DOI: 10.14256/JCE.1223.2015

CITATIONS
15

READS
7,607

2 authors:

Majid Pouraminian
Islamic Azad University
77 PUBLICATIONS **219** CITATIONS

SEE PROFILE

Mohsen Ghaemian
Sharif University of Technology
67 PUBLICATIONS **1,211** CITATIONS

SEE PROFILE

Primljen / Received: 24.1.2015.
Ispravljen / Corrected: 7.7.2015.
Prihvaćen / Accepted: 24.8.2015.
Dostupno online / Available online: 10.1.2016.

Shape optimisation of concrete open spandrel arch bridges

Authors:

Majid Pouraminian, Ph.D. candidate
Islamic Azad University
Science and Research Branch
Department of Civil Engineering
majid.pouraminian@gmail.com

Prof. **Mohsen Ghaemian**, PhD. CE
Sharif University of Technology, Tehran
Civil Engineering Department
ghaemian@sharif.edu

Scientific paper - Preliminary report

Majid Pouraminian, Mohsen Ghaemian

Shape optimisation of concrete open spandrel arch bridges

An open spandrel arch bridge is analysed in this paper. A computer code is written to create a model from geometrical data, so as to solve the optimisation problem. An optimum design procedure is conducted in the paper, and the total material volume of the bridge substructure is adopted as an objective function. The substructure includes the column and the reinforced-concrete arch. Finally, the optimization technique is implemented using the Simultaneous Perturbation Stochastic Approximation algorithm.

Key words:
arch bridge, open spandrel, Simultaneous Perturbation Stochastic Approximation algorithm, longitudinal section optimisation

Prethodno priopćenje

Majid Pouraminian, Mohsen Ghaemian

Optimalizacija oblika lučnih mostova s otvorenim nadlučnim sklopom

U ovom se radu analizira lučni most s otvorenim nadlučnim sklopom. Računalni kod je izveden za izradu modela na temelju geometrijskih podataka, a radi rješavanja problema optimalizacije. U ovom se radu provodi postupak optimalnog projektiranja, a ukupan obujam materijala ugrađenog u donji ustroj mosta usvaja se kao objektivna funkcija. Donji ustroj sadrži stup i armiranobetonski luk. Na kraju je proveden i postupak optimalizacije pomoću algoritma za istovremeno stohastičko predviđanje poremećaja.

Ključne riječi:
lučni most, otvoreni nadlučni sklop, istovremeno stohastičko predviđanje poremećaja, optimalizacija uzdužnog presjeka

Vorherige Mitteilung

Majid Pouraminian, Mohsen Ghaemian

Optimierung der Form von Stahlbetonbogenbrücken mit Überbauten offenen Querschnitts

In dieser Arbeit wird eine Bogenbrücke mit Überbau offenen Querschnitts analysiert. Dafür wurde ein Computercode zur Modellgenerierung aufgrund geometrischer Daten erstellt, um das Optimierungsproblem zu bearbeiten. Dabei wurde das Verfahren des optimalen Entwurfs angewandt und das gesamte Volumen des für den Unterbau benötigten Materials als objektive Funktion angenommen. Der Unterbau umfasst Stütze und Stahlbetonbogen. Ebenso wurde die Optimierung mittels des Algorithmus für gleichzeitige stochastische Störungsvorhersagen durchgeführt.

Schlüsselwörter:
Bogenbrücke, Überbau offenen Querschnitts, ISPP Algorithmus, Optimierung des Längsschnittes

1. Introduction

Arch bridges have several positive features which make them highly attractive to designers. These features are as follows, [1]:

- Material choice is rather unrestricted, as structure is suitable for various materials.
- Spans can vary up to 500 m in length, theoretically even more.
- Suitable for large relief surroundings.
- Aesthetically beautiful structures.
- Scouring does not occur because the bridge pier stands on the arch and under the bridge deck.

Features hindering the use of arch bridges are:

- In cases when long span are required, other bridge types are economically more attractive.
- Risk of buckling is higher in arch bridge compared to other bridge types.
- The cost of framework is high for large-span arches.
- The arch base should stand on a rocky and rigid subsoil.

The optimization of cable-stayed bridges is considered in [2, 3] and the cable stress and deck displacements are named as design constraints. Aydin et al. [4] studied the contribution of genetic algorithm to the bridge deck design optimization. None of the above mentioned studies applied SPSA (Simultaneous Perturbation Stochastic Approximation) algorithm. Baldomir et al. [3] used the MATLAB optimization toolbox to minimise the total volume of steel cables as an objective function. Togan and Daloglu [5] used the reliability-based design optimization (RBDO) for optimising the size of bridge-structure elements. Guan et al. [6] utilized the principal-stresses based evolutionary structural topology optimization method for optimization of the arch, tied arch, cable-stayed and suspension bridges, where the stress, displacement and frequency values were taken as constraints. Makiabadi et al. [7] applied the teaching-learning-based size optimization (TLBO) algorithm to optimise the size of real-life truss bridges. The majority of previous studies focused on the size (cross-section) and topology optimization of bridge-structure elements. This paper proposes a methodology for optimising the longitudinal shape of open spandrel arch bridges.

2. Bridge description

The Cetina Bridge was used as a case study. It is a long-span open reinforced concrete arch bridge spanning the Cetina River Canyon near the town of Trilj in Croatia. The arch measures 140 m in span and 21.5 m in rise, giving the rise-to-span ratio of 1/6.5. The aerial view of the Cetina Bridge is given in Figure 1. The materials used for building the Cetina River Bridge, without abutments and foundations, are shown in Table 1. The total reinforced concrete volumes used in the superstructure and substructure amount to 35 % and 65 %, respectively, while the total quantity of reinforced concrete used in the superstructure and substructure adds up to 32 % and 68 %, respectively [8].

The longitudinal layout of the Cetina River Bridge is shown in Figure 2. The 10-span continuous bridge superstructure consists of precast-prestressed concrete girders, cast-in-site deck plate, and cross-girders at supports only. The deck structure is supported by nine pairs of columns, six of which are connected to the arch (Figure 2). All dimensions are presented in meters. An 8.3 m long cap-beam transversely connects the columns. Columns are of box cross-section, 1.5 m x 1.8 m, with 30 cm thick walls, except for the highest columns which are located at the arch springing. Cross sections of individual columns were determined on the basis of stability calculations (Figure 3). The arch is fixed to the single-cell cross-section with constant outer dimensions of 5.5 m x 8.0 m (Figure 4). The concrete class C45/55 was adopted for the arch [8]. It can be seen in Table 1 that the greatest quantity of concrete was placed in the arch structure. While constructing the framework and concrete arch, a tower (with the height expressed as H) was established at both sides of the arch to which the framework keeping cables were joined. 12, 15, and 19 strand cables were predominantly used.

Figure 1. Aerial view of Cetina River bridge

Table 1. Material consumption at Cetina River bridge

Material consumption / Type of material		Quantity	Consumption
Concrete	Arch	1411 m^3	0.69 m^3/m^2
	Columns	615 m^3	0.30 m^3/m^2
	Prestressed T-girder	693 m^3	0.34 m^3/m^2
	Deck plate	445 m^3	0.22 m^3/m^2
Reinforcement	Arch	545.2 t	265.4 kg/ m^2
	Piers	196.1 t	96 kg/ m^2
	Prestressed T-girder	151.8 t	73.9 kg/ m^2
	Deck plate	193.7 t	94.3 kg/ m^2
Tendons	Prestressed T-girder	33.8 t	16.5 kg/ m^2

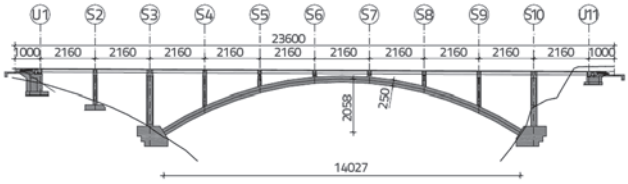

Figure 2. Elevation of Cetina River Bridge [8]

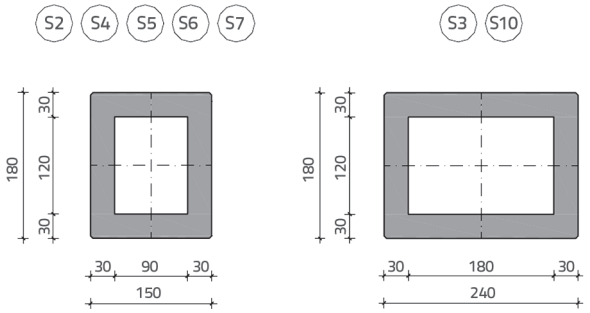

Figure 3. Cross section of bridge columns in substructure

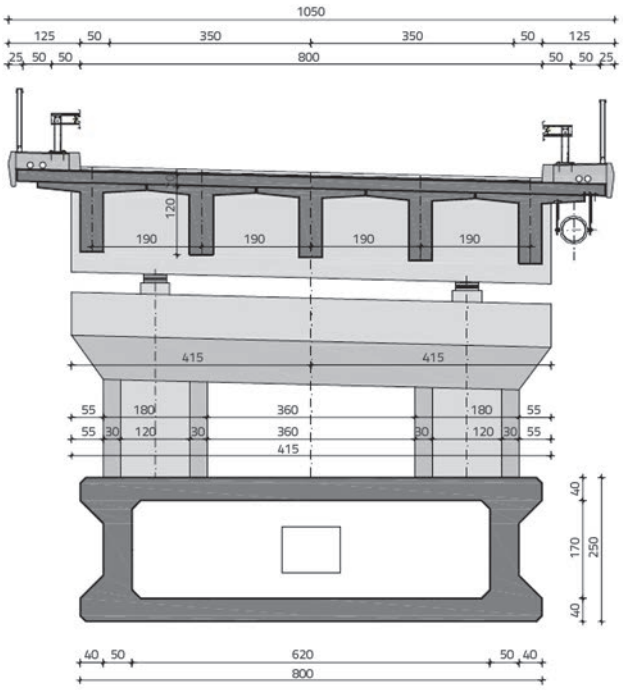

Figure 4. Arch and superstructure cross sections at Cetina River Bridge [8]

3. Optimization algorithm

The gradient-based Simultaneous Perturbation Stochastic Approximation (SPSA) algorithm, developed by Spall (1994), is a powerful algorithm that is used for optimisation of complex systems. One of the SPSA algorithm's features is that it requires only two structural analyses in each cycle of the optimization process, and this regardless of magnitude of the optimization problem. The accidental nature of this algorithm increases the probability of achieving the global optimization. The SPSA algorithm implementation stages are explained in six steps as follows, [9].

Step 1:
In this stage, the counter k = 1 is selected and the early X is produced by searching the space randomly. Non-negative constant values of a, c, A, γ, α, are the initializations. Then c_k and a_k values are calculated according to equations (1) and (2).

$$c_k = \frac{c}{k^{\gamma}} \tag{1}$$

$$a_k = \frac{a}{(A+k)^{\alpha}} \tag{2}$$

Step 2:
The production of the random Perturbation vector Δ_k should meet special conditions. Every n variable of this vector is independently produced using the probability distribution function with a zero mean value. The use of the Bernoulli ± 1 distribution, with the probability equalling to ½, is a simple and suitable choice for each entry. For example, $\Delta^T = \{-1,1,-1,1,-1,1,-1,1,-1,1\}$ is a sample of the vectors produced using the Bernoulli distribution with ten entries.

Step 3:
Upper and lower bounds of the function in a considered point are calculated for simultaneous perturbation of all entries in vector X, so as to produce the objective function; therefore $y(X_k+C_k\cdot\Delta_k)$ and $y(X_k-C_k\cdot\Delta_k)$ are measured by C_k and Δ_k as calculated in previous stages.

Step 4:
In this step, an approximate gradient of the function is calculated using equation (3). $G_k(X_k)$ is the approximate gradient of the function in iteration k of the optimization process, while Δ_{kj} is the entry j from the Δ_k vector.

$$\hat{G}_k(X_k) = \frac{y(X_k + c_k\cdot\Delta_k) - y(X_k - c_k\cdot\Delta_k)}{2\cdot c_k} \begin{bmatrix} \Delta^{-1}_{k1} \\ \Delta^{-1}_{k2} \\ \vdots \\ \Delta^{-1}_{kj} \\ \vdots \\ \Delta^{-1}_{kp} \end{bmatrix} \tag{3}$$

Step 5:
In this stage, the value X is updated by equation (4) using the approximate gradient from the previous step; therefore X_k is converted to X_{k+1} for calculation in the next stage.

$$X_{k+1} = X_k - a_k \cdot \hat{G}_k(X_k) \tag{4}$$

The calculated X is controlled so as not to exceed the allowable bound X. The allowable bounds are the boundary constraints

that should be controlled in each optimization step; therefore, X_{k+1} is approved by means of equation (5).

$$X^l \le X_{k+1} \le X^u \quad (5)$$

Where X^u is the upper bound, and X^l is the lower bound of the vector X. The X value should be corrected if it exceeds this boundary and the next step should be reached with the corrected value.

Step 6:
In this stage, the program stops if the number of allowable iterations is exhausted. Otherwise, steps 2 to 5 should be repeated. Finally, the least objective function value, for which all conditions were met during the optimization process, is considered as the optimized answer. The SPSA process used in an arch bridge optimization is shown in Figure 5 [10].

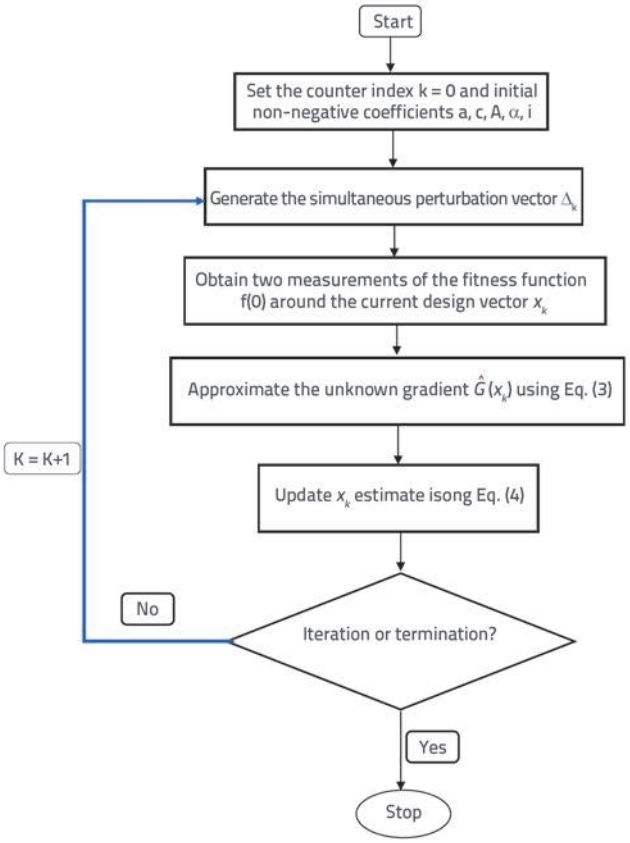

Figure 5. Simultaneous Perturbation Stochastic Approximation flowchart [10]

The shape optimization problem is to find the design variables X, while minimizing the objective function F(x) under the constraint functions $h_j(X)$ and $g_k(X)$, which can be stated mathematically as shown in equations (6) to (8):

$$\text{Find: } X = [X_1 X_2 \ldots X_n]^T,\ a_i \le X \le b_i \qquad (i = 1, \ldots, n) \quad (6)$$

To minimize F(x)

$$h_j(X) = 0 \quad (j = 1, \ldots, p) \quad (7)$$

$$g_k(X) \le 0 \quad (k = 1, \ldots, m) \quad (8)$$

Due to dependence of the bridge deck height on the road level, the deck height is assumed to be constant. In addition, the changes in concrete arch geometry lead to changes in bridge pier heights. A considerable amount of concrete was used in the bridge substructure. The component of the substructure is the column and arch with a single-cell section. Therefore, in this study, the concrete used in arch and piers was selected as the objective function, as shown in equation (9). Equations (10) and (11) were considered as tension constraints, equations (12) and (13) as functional constraints, and equations (14) to (17) as geometrical constraints.

$$V_{Substr.} = V_{Arch} + V_{Column} \quad (9)$$

Subject to:

$$\sigma_i \ge \sigma^c_{max} \qquad i = 1, 2, \ldots, nip \quad (10)$$

$$\sigma_i \le \sigma^t_{max} \qquad i = 1, 2, \ldots, nip \quad (11)$$

$$\delta_i \le \delta^v_{max} = \frac{S}{800} \qquad i = 1, 2, \ldots, nip \quad (12)$$

$$\delta_i \le \delta^h_{max} = \frac{H}{800} \qquad i = 1, 2, \ldots, nip \quad (13)$$

$$\frac{t_c}{t_L} - 1 \le 0 \quad (14)$$

$$\frac{t_c}{t_R} - 1 \le 0 \quad (15)$$

$$\frac{R_{Rint}}{R_{Rext}} - 1 \le 0 \quad (16)$$

$$\frac{R_{Lint}}{R_{Lext}} - 1 \le 0 \quad (17)$$

The value "n" indicates the number of design variables. The subscripts j, k, and i denote the number of equality constraints, behavioural constraints, and design variables, respectively. a_i and b_i are allowable bottom and top limits of the design variables that are introduced to deal with various requirements. This optimization does not contain the equality constraints. The value σ_i is the principal tensile stress in the i^{th} integration point, while σ^t_{max} and σ^c_{max} are the maximum allowable tensile and compressive stresses, respectively. "nip" is the total number of integration points in bridge arches elements, and S and H are the arch span length and tower height, respectively. The central deformation of the concrete arch span, and horizontal drift of the cable holding the tower, should not exceed the allowable value.

4. Finite element analyses

The stress and displacement constraints of the model must be controlled in the optimization algorithm, after every random

modelling of the bridge geometry. Once the geometry is modelled, the program analyses the bridge structure. The finite element model features utilized in each iteration are given in this part. A three-dimensional finite element model was developed for the purpose of the analysis. The main span and columns were simulated with two node elements (line elements) having three translational degrees of freedom (DOFs) and three rotational DOFs at each node. An eight node solid element was used for the reinforced-concrete non prismatic single cell arch. All elements were assumed to be linear iso-parametric elements. The full FE model consisted of 94 line elements, 252 solid elements, and 380 nodes. The main concrete arch is fixed at the abutments. In this study, only the linear elastic behaviour is considered and the optimized shapes and the arch web are not checked for buckling, material nonlinearity, and large deformation effects, [11].

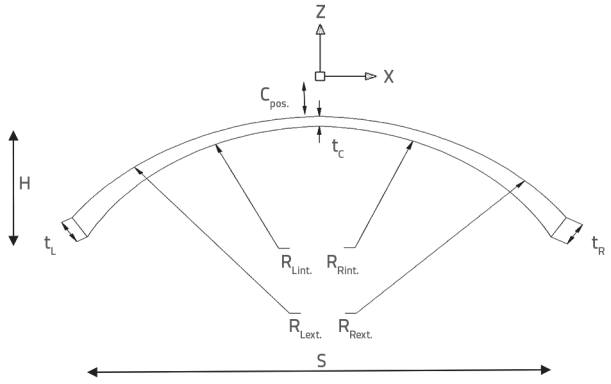

Figure 6. Arch geometry configuration, and definition of shape and design variables

5. Program description

The program was developed using the MATLAB code in order to generate node coordinates and then finite elements to model geometry of an arch bridge. Finally, the optimization technique was conducted using the Simultaneous Perturbation Stochastic Approximation (SPSA) algorithm. Parabolic conic functions were employed for defining the arch geometry in longitudinal sections.

The program includes four steps:

- Random generation of bridge parametric geometry by means of MATLAB
- Evoking the Finite Element Method Using ANSYS to analyse the construction
- shape optimization of the arch section and longitudinal profile
- Optimum design control under construction loads like the arch weight considering construction stages, traffic load and wind load.

The design variables are: height of skewback abutment ($\mathbf{t_L}$; $\mathbf{t_R}$), height of arch crown ($\mathbf{t_C}$), back and soffit radii of arch ($\mathbf{R_{Lext}}$; $\mathbf{R_{Rext}}$ and $\mathbf{R_{Lint}}$; $\mathbf{R_{Rint}}$), and position of crown with respect to global axes ($\mathbf{C_{pos}}$). According to the model shown in Figure 6, a bridge can be created by a vector X that has eight components including shape parameters of the arch bridge, as follows:

$$X = \{t_C; t_{AL}; t_{AR}; C_{pos}; R_{Lint}; R_{Rint}; R_{Lext}; R_{Rext}\} \quad (18)$$

The geometric description of bridge arches according to design variables is shown in Figure 6.

A computer code was written for both symmetrical and unsymmetrical shape optimization of arch bridges. Design variables were considered separately for the left and right sides of the bridge, abbreviated to L and R. The optimization aims to determine the optimized shape of the bridge arch. Hence, the pier-to-pier distance, and the girder and deck height values, are assumed to be constant. In the optimization process, the distance between the columns is assumed to be constant and equals to 21.6 m. Fair results are obtained when this model is used to compare the original design and the optimized one. Changes in pier-to-pier distances leads to the change in forces acting on the arch. Also, column cross sections are not taken as design variables. Instead of this, pier cross sections are selected proportionally with those of the application project. Most of the practical design variables and constraints are considered during problem formulation. Three types of design constraints are taken into account: stress constraints of the arch, transversal displacement constraints of the arch crown, and geometrical constraints. Appropriate limit displacement values are used for each bridge type. These values are determined based on the recommendations given in the Chinese Design Guideline for Highway Bridges, and in the Australian Bridge Code [12, 13] where the allowance for deflection under service load should not exceed 1/800 of the main span of the bridge [6]. Arch web thicknesses are not adopted as design variables. The shape optimization was made for each arch web thickness.

Different optimum volumes obtained for various web thicknesses are shown in Figure 7. 35 cm was adopted for web thickness as a constant design parameter in the optimization process. The high strength concrete and additional local reinforcement can be used to provide sufficient strength for cable anchoring into the arch web. The convergence rate of the objective function in the optimization process is shown in Figure 8. After the optimization process, the volume of substructure decreased by 30 % in comparison with the initial design. The optimized vector of design variables is given in equation (19).

$$X^{optimum} = \{1{,}8\ m;\ 2{,}5\ m;\ 2{,}5\ m;\ 0{,}36\ m;\ 117°;\ 117°;\ 120°;\ 120°\} \quad (19)$$

Obviously, the optimized design is symmetric for the symmetry between early geometry of the structure and loading. A half of the optimized arch is shown in Figure 9. The height to span

ratio is one of the parameters that are essential for structural performance of the arch. This value decreased from 0.147 in the original design to 0.136 in the optimized one. A 7.5 % decrease is observed with the reduction in arch length. The ratio of the arch middle section height to side section height is 1 in the original design and 0.7 in optimized design. In the optimized design, the middle section height decreases by 28 percent and no changes is observed in the side section. .

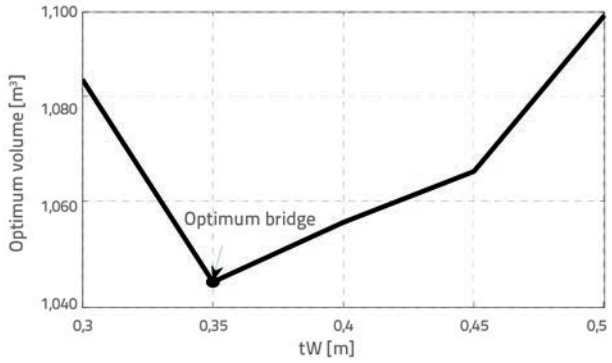

Figure 7. Optimum volume for different web thicknesses

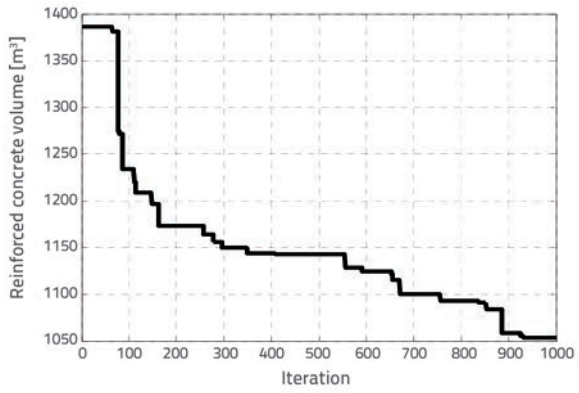

Figure 8. Convergence of bridge body volume

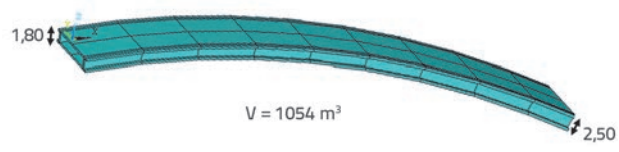

Figure 9. Optimum shape of bridge arches

6. Analysis of construction process

Failure of bridges during construction is an issue of high importance to bridge designers. Thus, an optimum arch shape, controlled for design loads during construction, is examined in this section. The optimized design strength should be controlled with regard to construction loads including sequential construction loading, live load, and traffic.

6.1. Design loads

The following three load types were considered in the sequential construction analysis of the bridge:

Dead loads: all dead loads were applied statistically in the negative Z-direction, as shown in Figure 6.

Live loads: Since the Cetina Bridge accommodates a two-lane roadway and 1.25 m wide sidewalks on both sides, the traffic and pedestrian loads are considered. For simplicity, the applied traffic loads are assumed to be uniformly distributed along the bridge deck. The design live load was assumed to be 5600 N/m [14, 15].

Wind loads: Wind loads for bridge design were determined on the basis of the Chinese Wind-Resistant Design Guideline for Highway Bridges. The girder and concrete arch are subjected to the following three wind load components: drag force (F_y), lift force (F_z), and pitch moment (M) , equations (20), (21) and (22).

$$F_y = \frac{1}{2}\rho V_z^2 C_y D \tag{20}$$

$$F_z = \frac{1}{2}\rho V_z^2 C_z B \tag{21}$$

$$M = \frac{1}{2}\rho V_z^2 C_M B^2 \tag{22}$$

In the equations, C_y, C_z and C_M are the coefficients for the drag force, lift force, and pitch moment, respectively; ρ is the air density; B is the width of the deck or arch rib; D is the vertical projected area of the deck or RC arch. V_z is the wind speed at the height of z, as given in equation (23):

$$V_z = \left(\frac{z}{10}\right)^{0,16} V_{10} \tag{23}$$

where V_{10} is the design wind speed at the height of 10 m. The design wind velocity at the height of 10 m, is taken to be 40 m/s. Three components of wind load acting on the bridge deck are shown in Figure 10.

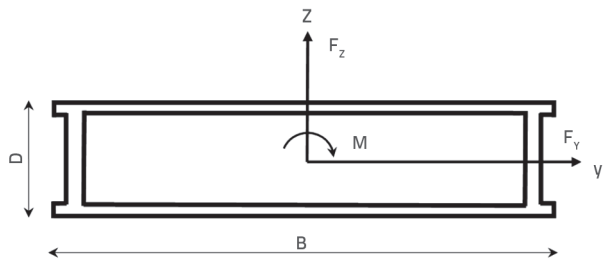

Figure 10. Three components of wind load acting on bridge arch

6.2. Modelling of construction sequences

The concrete arch was realized step by step. In each step, the steel cables were anchored to the steel tower and the formwork was restrained by two sides of the valley. In the staged construction simulation presented in this section, the principal tension stresses and displacement of the tower and concrete arch, did not overpass allowable values. Simultaneously, the probable wind load at the construction site was taken into account. A total of seven erection phases were considered in the numerical analysis. Detailed analyses of all construction phases were performed for one half of the arch due to symmetrical erection, with 8 segments for every half span and one closure segment. A 3D model is developed in this section using the finite element program, as well as the birth and death technique to simulate a sequential bridge construction. Structural analyses were conducted for all concrete arch and steel cable elements, as can be observed in the output of the finite element program. In each stage, if a part of the arch is concreted, its elements are considered alive, while other elements are considered dead. When an element is considered dead, it means that the element has no mass and is determined by the zero elasticity modulus.

A structural analysis is performed as well as a stress analysis assessment, which allows structural safety checking. Geometrical nonlinearity was induced in the analysis. Figure

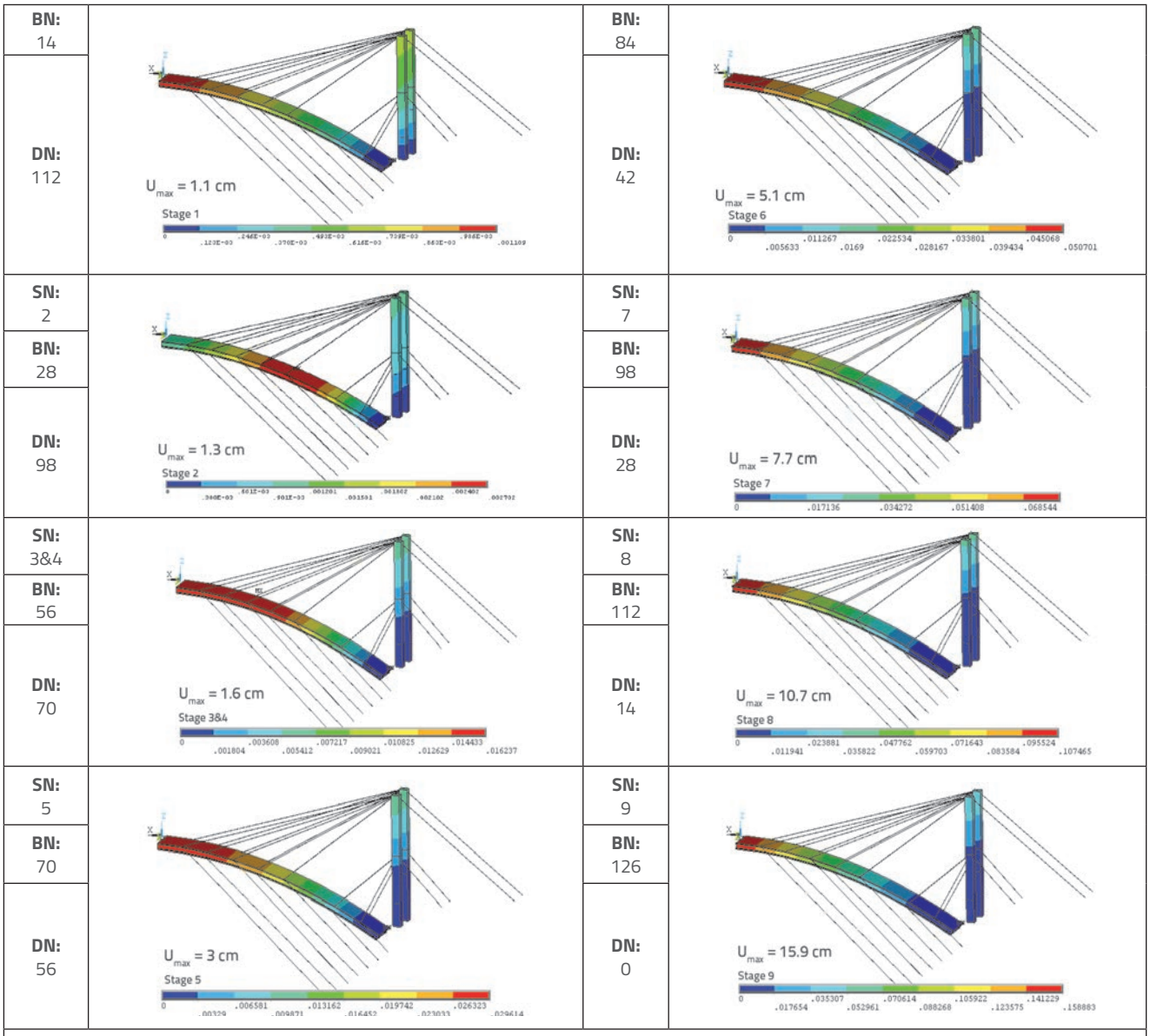

U_{max}: Displacement of Arch crest in Z direction due to stage construction and wind loads
Birth & Death elements: in each stage birth elements in right side and death elements in left side of arches
BN: Number of birth elements, **DN**: Number of death elements, **SN**: Stages number

Figure 11. Total displacement during erection

11 shows the total arch displacement in each phase, with the dead weight and wind load, which was strictly respected during bridge construction. As shown in Figure 11, the displacement of the arch end rise increases slowly by progressive placing and staged construction. Early concrete placing results in 1mm displacement and the displacement reaches 16 cm at one half of the arch, with restrained steel cables, which is smaller than the allowable deflection. The horizontal displacement of the tower is shown in Figure 12. The allowable displacement is determined based on recommendations given in the Chinese Design Guideline for Highway Bridges and the Australian Bridge Code [12, 13] where it is stated that the deflection allowance under the service load should not exceed 1/800 of the tower height. Also, all stresses during construction sequences should be lower than the allowable stress of the material [16].

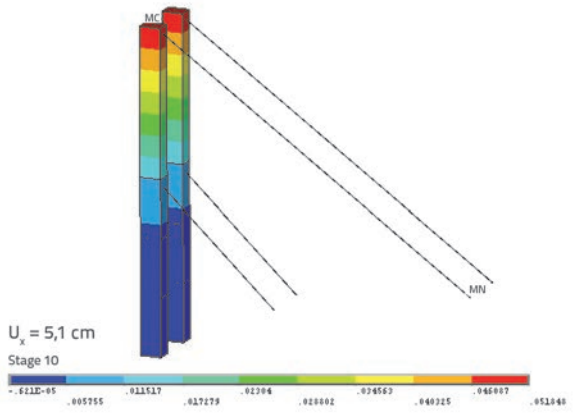

Figure 12. Horizontal displacement during erection

7. Conclusion

Results obtained by optimizing longitudinal section of an arch bridge are presented in this paper. The following conclusions can be drawn from these results:

- The computer code created allows changes on the finite element model (geometry, physical properties of material, boundary conditions, higher order element, flange thickness at the arch section and longitudinal section of the bridge) in a simple way. In addition, it permits inclusion of new load combinations in the optimization process.
- It was concluded that SPSA can be effectively used in bridge shape optimization procedures. The shape optimization process enables significant reduction in the weight of the structure. The total reinforced concrete volume obtained in this study has been reduced by 30 % compared to the application project. The minimum volume of substructure achieved was 1054 m^3 compared to 1504 m^3 in the application project.
- Constraints can easily be adapted to the problem using the penalty function and design variable sets.
- The height of the middle section, as related to the side section of the arch, should be less than 1 in such bridges.
- The concrete consumption decreases by reducing web thickness at arch sections; however any decrease below the web thickness of the arch section results in a non-economic program.

Also, any increase above the web thickness of the arch section results in a non-economic program.
This research can further be improved upon by:

- Considering buckling analysis of optimum design model with dead weight and wind loads.
- Considering material nonlinearity and large deformation effects in the analysis of structures.
- ncluding other structural elements such as the columns and pre-stressed T-girders as design variables in the optimization process.
- Including an optimum number of columns as design variables.

REFERENCES

[1] Hepola, I., Marwedel, R.: Arch Bridges, Aalto University, Rak-11.3001 Design of Bridges, 2012.

[2] Lute, V., Upadhyay, A., Kumar Singh, K.: Genetic Algorithms-Based Optimization of Cable Stayed Bridges, J. Software Engineering & Applications, 4(2011), pp. 571-578, DOI:10.4236/jsea.2011.410066

[3] Baldomir, A., Hernandez, S., Nieto, F., Jurado, J.A.: Cable optimization of a long span cable stayed bridge in La Coruna (Spain), Advances in Engineering Software, 41(2010), pp. 931-938. DOI: 10.1016/j.advengsoft.2010.05.001

[4] Aydin, Z., Ayvaz, Y.: Overall Cost Optimization of Prestressed Concrete Bridge using Genetic Algorithm, KSCE Journal of Civil Engineering, 17(2013)4, pp. 769-776. DOI: 10.1007/s12205-013-0355-4

[5] Togan, V., Daloglu, A.: Design and Reliability Based Optimization of a 2D Arch Bridge , Journal of Engineering and Natural Sciences, 25(1), pp. 17-26., 2006.

[6] Guan, H., Chen, Y.J., Loo, Y.C., Xie, Y.M., Steven, G.P.: Bridge Topology Optimization with Stress, Displacement and Frequency Constraints, Computer & Structures, 81(2003), pp. 131-145. DOI: 10.1016/S0045-7949(02)00440-6

[7] Makiabadi, M.H., Baghlani, A., Rahnema, H., Hadianfard, M.A.: Optimal Design of Truss Bridges using Teaching-Learning- Based Optimization Algorithm, International Journal of Optimization in Civil Engineering, 3 (2013) 3, pp. 499-510.

[8] Žderic, Ž., Runjić, A., Hrelja, G.: Design and Construction of Cetina Arch Bridge, Chinese-Croation Joint Colloquium, Brijuni Islands, pp. 285-292, 2008.

[9] Seyedpoor. S.M., Salajegheh. J., Salajegheh, E., Gholizadeh, S.: Optimal design of arch dams subjected to earthquake loading by a combination of simultaneous perturbation stochastic approximation and particle swarm algorithms. Journal of Applied Soft Computing. 11(2011); pp. 39–48. DOI: 10.1016/j.asoc.2009.10.014

[10] Pouraminian, M., Pourbakhshian, S.: SPSA Algorithm Based Optimum Design of Longitudinal Section of Bridges. Indian Journal of Science and Technology, 7 (2014) 9, pp. 1327-1332.

[11] Ministry of Communications of People's Republic of China, Specifications for Design of Reinforced Concrete and Prestressed Concrete Highway Bridges and Culverts (JTJ023-85), China Communications Press, Beijing, 2003.

[12] AustRoad. 92, AustRoad Bridge design code. NSW: Australian Railway Association,1992.

[13] AASHTO, Standard specifications for highway bridges, American Association of State Higway and Transportation Officials, Washington, D.C. 2002.

[14] Cheng, J., Li, Q.S.: Reliability analysis of long span steel arch bridges against wind-induced stability failure , Journal of Wind Engineering and Industrial Aerodynamics, 97(2009), pp. 132-139. DOI: 10.1016/j.jweia.2009.02.001

[15] Xiang, H.F., Chen, A.R., Lin, Z.X.: An introduction to the Chinese wind-resistant design guideline for highway bridges, Journal of Wind Engineering and Industrial Aerodynamics, 74 -76(1998), pp. 903-911. DOI: 10.1016/S0167-6105(98)00082-8

[16] Mahmud, H.M.I., Omar, M.A.: Effects of construction sequences on a continuous bridge, IABSE-JSCE joint conferences on advances in bridge engineering-II, Dhaka, Bangladesh, pp. 191-200, 2010.